Exploration of cyclopropyl radical ring opening to allyl radical by Newton trajectories: importance of valley-ridge inflection points to understand the topography

Wolfgang Quapp · Josep Maria Bofill · Antoni Aguilar-Mogas

Abstract Valley-ridge inflection points (VRI) on the potential energy surface for the ring opening of the cyclopropyl radical to allyl radical are determined using the tool of Newton trajectories (Quapp and Schmidt in Theor Chem Acc 128:47, 2011). VRIs play a role in the understanding of bifurcating reactions. The region where the bifurcation takes place is usually governed by a VRI point. For this important ring opening, the knowledge of the VRI point after the transition state was demanded some years ago (Mann and Hase in J Am Chem Soc 124:3208, 2002). Because the transition state is not symmetric, also the steepest descent from the transition state is not along a symmetry axis, and in such cases the steepest descent can fail the VRI point. That is the case here, indeed, though the pathway of the steepest descent goes near to a VRI point downhill. However, an electronic intersection seam disturbs the relations. The exploration of the notorious curvilinear potential energy surface of this ring opening has delivered some further VRI points, which are reported. They give a frame for possible ring-opening channels including the conrotatory case.

W. Quapp (✉)
Mathematisches Institut, Universität Leipzig,
PF 100920, 04009 Leipzig, Germany
e-mail: quapp@uni-leipzig.de
URL: http://www.mathematik.uni-leipzig.de/MI/~quapp

J. M. Bofill
Departament de Química Orgànica, Universitat de Barcelona,
c/Martí i Franquès, 1, 08028 Barcelona, Spain

A. Aguilar-Mogas
Departament de Química Física, Universitat de Barcelona,
c/Martí i Franquès, 1, 08028 Barcelona, Spain

J. M. Bofill · A. Aguilar-Mogas
Institut de Química Teòrica i Computacional,
Universitat de Barcelona (IQTCUB), c/Martí i Franquès,
1, 08028 Barcelona, Spain

1 Introduction: the theory of Newton trajectories and bifurcation points

The concepts of potential energy surface (PES), reaction path (RP), and its more restrictive definition minimum energy path (MEP) are the basic grounds of many theoretical chemistry theories and models [1, 2]. The RP is defined as a continuous curve in coordinate space, which connects two minimums of the PES by passing through a first order saddle point (SP), also called transition structure (TS), of the PES. The energy of the SP is assumed to be the highest value tracing along the RP. The chemical kinetic theories are based implicitly or explicitly on this definition. Many different curves satisfy the RP definition. This is the reason of a variety of curves used for this purpose. The most common used are the steepest descent (SD) or gradient path [3], gradient extremals (GE) [4–6], reduced gradient following (RGF) [7–14] and its equivalent definition, the so-called Newton trajectories (NT) [15]. If the NT is completely located in a valley region, then this RP meets the category of MEP. That a curve type used as an RP representation becomes MEP is possible for different mathematical definitions.

An important feature of the PES is that a valley or a ridge can bifurcate. The fact is related to the existence of valley-ridged inflection (VRI) points [15]. A VRI point is a point in the configuration space where, orthogonally to the gradient, at least one main curvature of the PES becomes zero. The gradient itself is assumed to be not the zero vector. If additionally the gradient is zero, then a stationary point and a VRI point coincide [16]. It is important to take into account that VRI points, which are defined in this way, are given independently of a curve definition of the RP representation. The VRI points are features of the PES under consideration. On the other side, a branching point or bifurcation point (BP) of a curve selected as a representation of an RP is a point where the curve branches. Usually such points do not coincide with a VRI point except for special NTs. The NTs branching at a VRI point are called singular NTs. The great remainder are regular NTs, which also do not bifurcate.

The VRI points can be classified into two main classes. A valley starting from an SP can bifurcate downhill and the two branches can lead to two valleys with their corresponding minimums. Between the two valleys a ridge emerges. Then, the VRI point is a valley-pitchfork (vpVRI) bifurcation. Or, a valley starting from a minimum can bifurcate uphill and the two branches can lead to two SPs. Between the two valleys, again a ridge emerges leading usually to an SP of index two. Then, the VRI point is also a vpVRI bifurcation. There is another possibility that a ridge on the PES bifurcates into two ridges going uphill, and between the two ridges emerges (in the chemical "interesting" case) a valley. The VRI point is a ridge-pitchfork (rpVRI) bifurcation. A possibility, which is not as interesting from the point of view of chemistry, is that in between a ridge of index 2 emerges—in cases with a PES of more than two dimensions. A further unusual possibility is that the VRI point is of a valley-ridge touching kind. The last possibility is the border-line case due to flat branches. So to say, its character is of a mixed type [15, 17]. The possibilities, vpVRI and rpVRI (interesting and may be not so interesting cases of higher index), as well as the mixed type, will emerge on the PES of the cyclopropyl radical ring opening, which is analyzed throughout the article.

Between a minimum and an SP of index 1, there are infinitely many regular NTs. However, between a minimum and an SP of index 2 is one singular NT that also crosses the VRI point in between. In Ref. [18] an iteration is proposed to find exactly the one singular NT using an empirical variational approach. We use the method throughout this article. With an initial choice of a search direction, we calculate by predictor and corrector steps an NT starting from a minimum, or an SP into the region of the guessed VRI. NTs are continuous curves which we represent by nodes in certain distances. The steplength of the predictor step prescribes the distance. Connecting all nodes of the NT with the guessed VRI and dividing the lines into further nodes, we test for all nodes the value of norm $|\mathbf{Ag}|$ and use the node with the minimal value for the new VRI point. Note that at the VRI point holds $|\mathbf{Ag}| = 0$. $\mathbf{A}$ is the adjoint matrix to the Hessian, and $\mathbf{g}$ is the gradient of the PES. The gradient at the guessed VRI is then used for the new search direction for a new NT run, and so on, up to convergence. Of course, the key always is an appropriate guess of the VRI region, at the beginning. The method is coupled with the GAMESS-US program[1] for the calculation of energy, gradient, Hessian matrix, and metric matrices in non-redundant, internal z-matrix coordinates. All this is used at every node without any updating, see also the web-page [21] for the programs on the VRI-propose [18].

2 Thermal ring opening of cyclopropyl radical into allyl radical

In Organic Chemistry and Chemistry, in general the prediction of stereochemistry of the electrocyclic ring-opening reactions, such as cyclopropyl radical, has been a long-standing question. For cyclic molecular structures in their ground state with an even number of electrons, these reactions are governed by the Woodward-Hofmann rules [22–24]. These rules predict either a conrotatory or disrotatory stereochemistry evolution depending on the orbital diagram associated with the system. For the cyclopropyl radical, a system with an odd number of electrons, the Woodward-Hofmann rules predict that both the conrotatory and the disrotatory stereochemistry evolution is nominally forbidden [25]. In the computational study reported in Ref. [25], a highly asynchronous transition structure with C_1 symmetry was identified. In a later computational study at the B3LYP/6-311G(2d) level of theory [26], the calculations of the RP represented as Intrinsic Reaction Coordinate (IRC) were carried out from the C_1 transition state to the allyl radical, concluding that the overall reaction occurs with disrotatory stereochemistry. Nevertheless, it is not possible to conclude from the IRC study that from an asymmetric transition state the disrotatory stereochemistry is favored. To clarify this question, Mann and Hase carried out dynamical calculations [27, 28]. The study of dynamics was carried out with a limited number of trajectories, but the authors conclude that with a large ensemble of trajectories one may predict no stereochemical preference for the ring opening. To explain this result, the authors argue that the possible existence of a VRI point along the PES region is associated to the ring-opening process. More recently, an

---

Fig. 1 Orbitals of the minimum M_c: σ double-occupied, n single-occupied, σ^* un-occupied
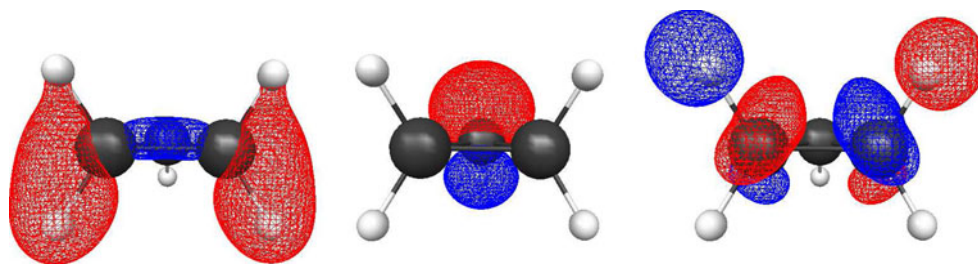
Fig. 2 Orbitals of the minimum M_a: π_1 double-occupied, π_2 single-occupied, π_3 un-occupied
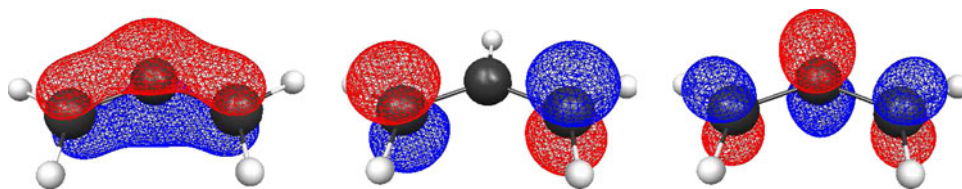
IRC analysis of this reaction concludes that there exists a VRI point near the IRC curve, and this VRI point is located in a ridge that divides the initial valley in two valleys each one related to the allyl radical [29]. Although the result reveals the existence of the hypothetical VRI, it is not complete conclusive because the VRI point is located in a non-symmetric bifurcation valley due to the fact, as explained above, that the transition state is not symmetric. Recently, it has been proved computationally and experimentally for ion alkali halo-alkane molecular systems that the existence of VRI points and bifurcating valleys on their PES have strong relations to their dynamics behavior and product ratios of this type of molecular systems [30].

The purpose of the present study is both to give a more detailed structure and features of the UHF PES (unrestricted Hartree-Fock) related to the ring opening of cyclopropyl radical and the potentiality of the NTs as a tool to view and analyze a PES. More specifically and with a concrete problem, we start with the following question: the localization of the transition state and the RP on the PES imposes the condition that the path at some points loses the symmetry of allyl and cyclopropyl radicals; this implies that there exist bifurcation points where it happens. How the NT curves perform the localization of these special pathways through the bifurcation points represents a real challenge. Note that we take NTs in valley regions as RP models.

As a starting point of this task, we have proved many initial guesses of NTs computed at the UHF/6-31G(d) level of theory (for reasons of cost) where at least some of them should be related to the conrotatory and disrotatory interconversion modes. However, we did not find NT pathways with the features related to the pure conrotatory or disrotatory motion. These results are in accord with the findings of Ref. [25]. An RP does not exist in the ground electronic state joining the minimums associated with allyl and cyclopropyl radicals, and preserving pure conrotatory or disrotatory motion. It is equivalent that the thermal conrotatory and disrotatory reactions are forbidden.

For the present purpose, we take the UHF/6-31G(d) level of theory as a way to generate the PES associated with the electronic ground state of the system. This wave function is very flexible and not very expensive from a computational point of view, also its solutions reasonably approach to the corresponding CASSCF wave function solutions (complete active space SCF) [31, 32]. The same type of wave functions was used in Ref. [25, 27–29] in the study on the cyclopropyl ring-opening system, see also Figs. 1 and 2. As explained very well in Ref. [25] it is interesting and important to analyze at different points of the PES the expectation value of the spin-squared operator S^2, $\langle S^2 \rangle$, of the UHF wave function. This magnitude in the present system indicates the spin contamination of states of higher multiplicity (i.e. quartet, sextet, …) to the doublet state multiplicity. Normally, in the points of the PES where $\langle S^2 \rangle$ differs from the value of the pure doublet wave function namely, 0.75, the UHF wave function shows a spin contaminant mainly due to the quartet state. If one uses the single-configuration approach, then the wave function of the quartet state can be written as a linear combination of three Slater determinants where each determinant is characterized by three molecular orbitals. These three molecular orbitals are related in some way with the σ double-occupied, n single-occupied, and σ^* un-occupied of cyclopropyl molecular orbital system, Fig. 1, and with the π_1 double-occupied, π_2 single-occupied, and π_3 un-occupied orbitals of the allyl π-molecular orbital system, Fig. 2. We refer to these molecular orbitals as ϕ_1, ϕ_2, and ϕ_3 in a generic form. The σ and σ^* molecular orbitals are related to the CC bond of the cyclopropyl radical to be broken in the evolution to the allyl radical, they are located in this bond, whereas the n orbital is the

single-occupied molecular orbital located at the methine group,—C1H4, of cyclopropyl molecular system.

According to these results, the ring-opening system is minimally well described by three electrons and three orbitals, namely, ϕ_1, ϕ_2, and ϕ_3 whereas the rest of electrons acts as a core potential. Due to this fact, the CASSCF wave function capable to describe this reaction adequately should be constructed using three electrons distributed within the above three molecular orbitals and the rest of electrons acting as spectators [25].

Nevertheless, in this extensive study of the PES we have found points and regions where the above electronic description is not enough, in addition to the three mentioned electrons, some core electrons are necessary to obtain a correct electronic description. These points have been associated with intersection points of the ground state with the PES of an excited electronic state; for this compare a work for cyclopropyl iodide [33]. The Born-Oppenheimer approximation assumes that the electrons relax instantaneously to their lowest energy distribution. For intersecting PESs, the situation becomes different. Because the electrons are strongly quantum mechanical, the transition cannot be a slowly "cooling" but has to be an ultrafast process that occurs at molecular geometries where the electronic states are isoenergetic [34, 35]. The geometries constitute a conical intersection and can be thought as the TS in the relaxation of the electronic excited molecule. However, they are not isolated points. Rather, they are collections of geometries that form a higher dimensional seam.

The molecular structure and the orbitals computed at UHF/6-31G(d) level of theory for the minimums of cyclopropyl and allyl radical are given in Figs. 1 and 2. The internal coordinates are reported in appendix in Tables A1 and A 6. The atoms numbering in an opened structure is given in Fig. 3. This and the z-matrix are used throughout the present study. The GAMESS-US suite of programs has been used for the calculations [19, 20].

The used z-matrix is

Cyclopropyl radical <– –> allyl radical						
C1						
c1						
c2	1	r1				
c3	1	r2	2	c2c1c3		
h4	1	hc1	2	hcc1	3	dih1
h5	2	hc2	1	hcc2	3	dih2
h6	3	hc3	1	hcc3	2	dih3
h7	2	hc4	1	hcc4	3	dih4
h8	3	hc5	1	hcc5	2	dih5
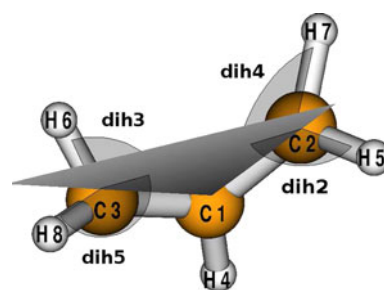
Fig. 3 Ring opening of the cyclopropyl radical: numbering of atoms in the z-matrix

3 The cyclopropyl radical bowl

In Table 1, we report a condensed version of the coordinates of all interesting structures, beginning with the cyclopropyl radical minimum, M_c, at UHF/6-31G(d) level of theory. The index c is used for points of the cyclopropyl part. This geometry structure belongs to the C_s point group of symmetry, and due to this fact the distance r1 is equal to r2 and the dihedral angles satisfy the relation dih2 = −dih5 and dih3 = −dih4. With the dihedral that involves the H4 atom, this set of coordinates is the most important and relevant in the changes of the molecule. The remainder of pairs of geometry parameters also preserves the C_s symmetry relation. The numbering of the two methylenes is interchangeable. Thus, in the present study we will very often treat the corresponding pairs of coordinates, also if the molecular structure does not belong to the C_s point group of symmetry, but they hold their connection to the other corresponding part.

From the minimum M_c, two "reaction directions" emerge. One is the 1D transit of the single methine hydrogen, H4, through the symmetry plane of the carbons, thus the dihedral angle goes through $\pm 180°$ [36, 37]. There is an SP_{H4} of the PES, see in the appendix Table A2. The remainder of the coordinates stays nearly unchanged at the minimum values.

The other possibility is the ring opening of the M_c structure by increasing the angle C2C1C3, which is equivalent to the bond breaking C2C3. The bond angle C2C1C3 will be our reference coordinate in the figures, so to say, it will be our reaction coordinate. The reaction may start in the symmetric subspace of all corresponding coordinate pairs of minimum M_c, thus there is, at least a 3D, subspace of important possibilities for the pairs r1 = r2, dih2 = −dih5, and dih3 = −dih4. We note that the z-matrix has 18 internal coordinates that we can decompose as follows, seven pairs each pair being related by the C_s symmetry, the C2C1C3 bond angle and the three coordinates of the H4 atom. Note: if the dihedrals

Table 1 Energies and special coordinates of stationary and VRI points on the PES of cyclopropyl radical opening to allyl radical (for UHF 6-31G(d))

point	Energy	r1[a]	r2	∠	dih1	dih2/dih4		dih3/dih5	
	au	C2C1	C1C3	CCC	H4[b]	H5/H7[b]		H6/H8[b]	
M_c	−116.41492	1.471	1.471	63.5	±120.2[c]	106.1	−107.5	107.5	−106.1
SP_{H4}	−116.40935	1.456	1.456	63.4	±180.0	106.3	−106.3	106.3	−106.3
VRI_{H4}	−116.36293	1.464	1.464	84.7	−148.0	97.0	−99.3	99.3	−97.0
SP_{i2}	−116.34794	1.448	1.451	90.8	−179.9	89.1	−89.2	89.2	−89.2
VRI_c	−116.37773	1.451	1.451	79.9	−132.9	108.5	−100.0	100.0	−108.5
SP_{ca}	−116.37268	1.416	1.471	86.7	−127.6	114.8	−71.5	87.0	−95.7
SP_{ca}		1.471	1.416	86.7	−127.6	95.7	−87.0	71.5	−114.8
SP_{ca}		1.471	1.416	86.7	127.6[d]	87.0	−95.7	114.8	−71.5
SP_{ca}		1.416	1.471	86.7	127.6[d]	71.5	−114.8	95.6	−87.0
VRI_{ca}	−116.37565	1.401	1.488	93.6	−127.2	120.7	−58.4	76.3	−89.2
VRI_{ca}		1.488	1.401	93.6	−127.2	89.2	−76.3	58.4	−120.7
VRI_r	−116.37204	1.403	1.503	97.8	−140.9	97.8	−76.1	80.6	−82.6
VRI_r		1.503	1.403	97.8	−140.9	82.6	−80.6	76.1	−97.8
VRI_s	−116.30119	1.458	1.458	108.7	−180.0	82.3	−82.3	82.3	−82.3
SP_{d1}	−116.37394	1.478	1.470	117.0	−180.0	78.9	−78.9	82.2	−82.2
SP_{d1}		1.470	1.478	117.0	−180.0	82.2	−82.2	78.9	−78.9
VRI_{rl}	−116.42231	1.316	1.470	115.5	−172.0	168.6	−7.8	102.8	−85.1
VRI_{i2}	−116.37769	1.459	1.456	124.1	−176.2	93.8	−85.3	85.5	−93.7
SP_{i2}	−116.37782	1.473	1.473	124.7	−180.0	91.6	−91.6	91.6	−91.6
VRI_a	−116.44217	1.407	1.407	128.3	−179.9	152.2	−39.1	39.1	−152.2
SP_{aa}	−116.43851	1.326	1.479	124.8	−180.0	180.0	0.0	97.3	−97.3
SP_{aa}		1.479	1.326	124.8	−180.0	97.3	−97.3	180.0	0.0
M_a	−116.46810	1.390	1.390	124.6	−180.0	180.0[e]	0.0	0.0	−180.0
M_a		1.390	1.390	124.6	−180.0	0.0	−180.0	180.0	0.0

[a] See Fig. 3 for numbering of the atoms. A subscript c is used for the symbols of the points in the cyclopropyl radical bowl, but a subscript a is used for points in the allyl radical bowl; see the text for further symbols

[b] C1H4 is the methine, C2H5H7 is methylene 1, and C3H6H8 is methylene 2

[c] Transition of sign changes the H atom numbering only

[d] For comparison, the two other symmetrical dih1-forms are added. Corresponding symmetrical forms also concern other points

[e] The first M_a is the disrotatory minimum, the second one the conrotatory

are involved, then a change of the molecule in the symmetry subspace C_s is a disrotatory change of the two methylenes.

We try to find the true singular NT in the 3D subspace in order to explore the PES from M_c to the bifurcation point. To do this, we start with some test calculations. One should take into account that NTs can turn back to the minimum, after passing a so-called turning point (TP) [38]. Or, if they start at the SP, they can turn up and go lost anywhere in the mountains of the PES. Due to this fact, one needs at least an NT which connects M_c with the SP_{ca} (their coordinates are in appendix Table A1). The true iteration of VRI_c by our program can begin if an NT with a kink indicates a neighborhood of the bifurcation. The present case shows a special difficulty, because the criterion |**Ag**| does not show

a tendency to go to zero [39] also in a small neighborhood of the VRI_c. At least, it emerges that the function |**Ag**| is very steep along the found singular NT to VRI_c, which is depicted in Fig. 4.

At this point, we make the following note with respect to the representation. We use both dih2 and −dih5 up to VRI_c because they are identical. However, after the VRI point, they bifurcate and go through different values and describe the behavior of the unsymmetric reaction path. (If we accept that the singular NT can be a description of an RP.) But we could renumber the molecule; then dih2 becomes −dih5, and vice versa. An analog argument concerns the coordinates dih3 and −dih4, as well as the two distances of the C-atoms, r1 and r2. The representation of Fig. 4 (left panel) means that we have the two
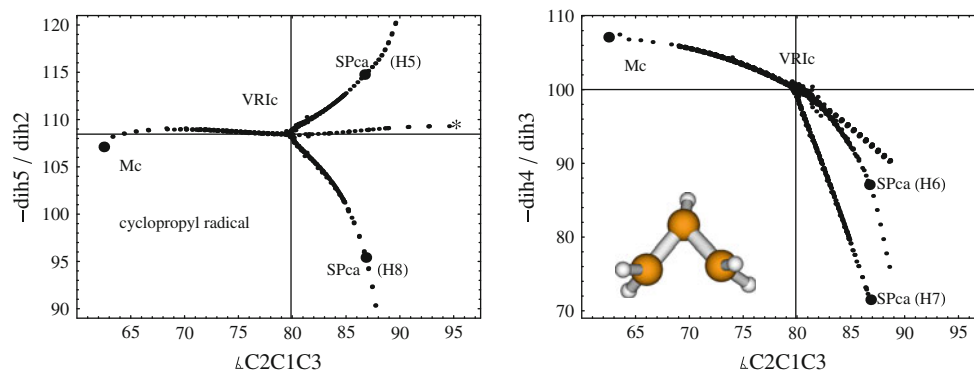
Fig. 4 The VRI point, VRI_c, of the pre-transition-state symmetry break for the ring opening of cyclopropyl radical indicated by the singular NT and its bifurcation point, see text. The *cross of grid lines* is the exact location of VRI_c. *Left* the representation uses the doubling of all points for coordinates dih2, as well as −dih5, to the same bond angle coordinate C2C1C3. The dihedrals are interchangeable. The associated H atoms are one possibility. Symbol *asterisk* is a point at the end of one PES, and an electronic intersection happens with another PES. *Right* The same singular NT through VRI_c for coordinates dih3 and −dih4. The inlay is the geometry of VRI_c

interchangeable coordinates of the transition states, SP_{ca} H(5) and SP_{ca} H(8), in one picture. If the upper one at the left panel concerns dih2, then the lower one concerns −dih5, or vice versa. An analog representation is used for dih3 and −dih4 at the right-hand side. The interchange of the dihedrals, correspondingly, results in the two different versions of SP_{ca} in Table 1. The double representation is helpful especially in cases where one branch of a bifurcating NT is hidden by the used projection in any coordinate plane, compare the right panel of Fig. 4.

Starting at the minimum, M_c, the singular NT has symmetric nodes up to the valley-ridge inflection point, VRI_c. The pathway is a valley of a small disrotatory behavior of the two methylenes along the ring opening, which bifurcates at VRI_c, and two different valleys go further uphill to the two SPs with C_1 symmetry, named SP_{ca}. Thus, the VRI_c is truly a vpVRI. At the SP, we find an asynchronous torsion of the two methylene groups. The central branch of the singular NT goes strong uphill in energy as a symmetric ridge belonging to the C_s symmetry. The energies of the last nodes of the ridge are so high, that it can be assumed that any reaction goes along the SPs of the first order. Because the two SPs are not symmetric as shown in Table 1, the valleys leading to them are also not symmetric. The symmetry C_s is lost at the bifurcation point. It is a dramatic difference between the left and the right panel of Fig. 4. The outgoing coordinate paths are not equal in these valleys. Nevertheless, the combination of either of the two valley branches with the pathway from M_c to VRI_c is a full RP from minimum M_c to SP_{ca}. This RP looses its initial symmetry. The present case contradicts the old picture of the conservation of nuclear symmetry along every RP (understood as a steepest descent path), compare [40]. For each of the two RPs, it is necessary to destroy the initial molecular symmetry of M_c to arrive at the corresponding SP_{ca} [25].

When the upper branch of the left panel of Fig. 4 concerns coordinate dih2 being related to H5, and consequently, when the lower branch of the same panel in Fig. 4 concerns with the coordinate −dih5 which belongs to H8, and dih2 becomes larger but dih5 becomes smaller, then the evolution from VRI_c to SP_{ca} occurs through a conrotatory change. The two hydrogens move simultaneously to the left-hand side in Fig. 1. With a similar observation and reasoning, when the upper branch of the right panel of Fig. 4 concerns with the coordinate dih3 being related to H6, and when the lower branch of the right panel of Fig. 4 is coordinate −dih4 which belongs to H7, and both dih3 and dih4 become smaller, then the evolution from VRI_c to SP_{ca} occurs through a (something disturbed) disrotatory character. The two hydrogens turn to an outer space, in Fig. 1. The view of the whole process means that the methylene 1 related to C2 rotates clockwise, whereas the methylene 2 related to C3 is compressed, because H6 and H8 approach in a concerted kind. Note: the "four" SPs in Fig. 4 concern one and the same structure of the cyclopropyl radical, correspondingly, to the four dihedral coordinates used.

It is important at this point to note that here emerges the intersection problem of excited PESs within the UHF methodology for the first time: An intersection point along the singular NT is indicated by a * symbol in the left panel of Fig. 4. It says that the structure, number, and occupancy of UHF natural orbitals with fractional occupancy has changed. Generally, we use the UHF methodology rather than CASSCF; however, the UHF methodology is not appropriate in the * region. We cut the calculation of the NT at this point. An expected symmetric SP of index 2 could not be reached going along this branch, because of the intersection with another PES.
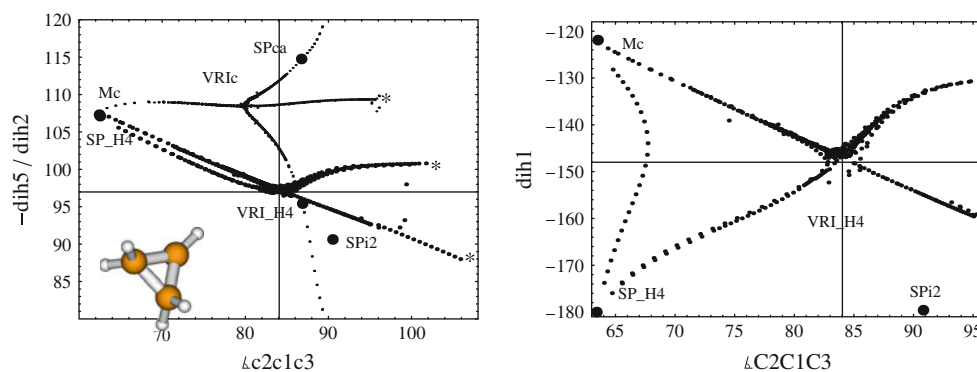
Fig. 5 *Left* The VRI point, VRI$_{H4}$ marking the border between two regions of attraction of the interesting SPs of cyclopropyl radical. It is indicated by the singular NT and its bifurcation point. The *grid lines* cross depicts to the location of VRI$_{H4}$. Symbols *asterisk* are points at the end of this UHF PES. For comparison, the singular NT of VRI$_c$ is also given by thin points, see Fig. 4. The inlay is the geometry of VRI$_{H4}$. *Right* VRI$_{H4}$ for coordinate dih1. The additional *left* NT is a regular one between M$_c$ being *left top*, and SP$_{H4}$ being *left bottom*
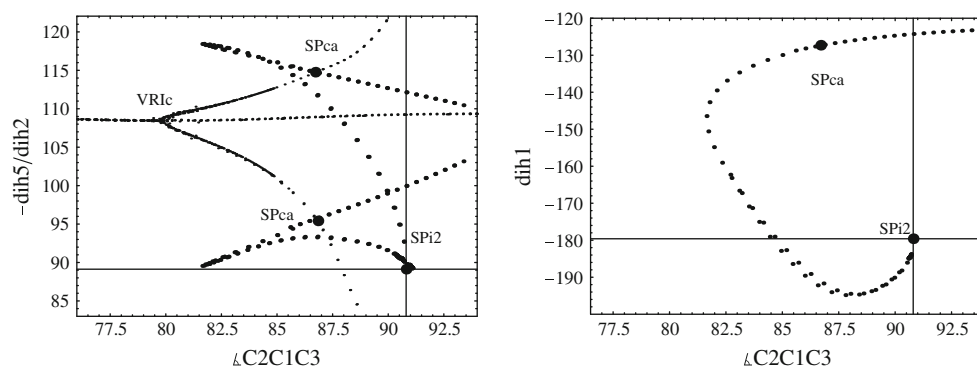
Fig. 6 *Left* a regular NT to SP$_{i2}$ for coordinates dih2 and −dih5. Compare the caption of previous Figures. The VRI$_c$ system is given in the *left panel* by thin points, for comparison. *Right* The same regular NT to SP$_{i2}$ for coordinate dih1

The border between the regions where NTs going to SP$_{H4}$, or others going to an SP$_{ca}$, is marked again by a singular NT which bifurcates at a symmetric bifurcation point in C$_s$, the VRI$_{H4}$, see appendix Tables A2. It is demonstrated in Fig. 5 where additionally to the dihedrals dih2 and −dih5, also the behavior of dih1 is shown. It is clear that here the bifurcation mainly concerns the coordinate dih1 in a plane with the bond angle C2C1C3. There is experimental evidence that the lone H4 of the C1H4 bond can tunnel through the barrier of SP$_{H4}$, if the cyclopropyl radical is vibrationally exited [37]. One should hold in mind the fact along the full ring opening.

Looking at the left panel of Fig. 5, the singular NT through VRI$_{H4}$ meets "with an accident" because the two bifurcating branches are no mirror pictures, like in other bifurcations. The character of the VRI$_{H4}$ is of the mixed type, thus it is neither vpVRI nor rpVRI. The two upper branches in Fig. 5 are valleys of the PES, but the two lower branches are ridges of index one. The two kinds of curves have a kink and "touch with the kink" at the VRI point [15, 17]. However, the name VRI may be correct: if we look at

the right panel in Fig. 5, there the straight line from M$_c$ in the left upper corner to the right lower region describes a valley-ridge inflection, as well as the two branches which connect the SP$_{H4}$ in the left lower corner with the right upper region describe a ridge-valley transition.

The two right branches meet after the VRI$_{H4}$ at points that intersect with the PES of an excited electronic state. That is the reason that a possible connection to SP$_{ca}$ could not be shown.

In Fig. 5 we also show the location of an SP of index two, SP$_{i2}$ on the PES of the M$_c$ bowl. The Hessian matrix of this SP was computed using GAMESS-US [19, 20], and the corresponding diagonal representation shows two negative eigenvalues. Figure 6 shows a regular NT connecting the SP$_{ca}$ with this SP$_{i2}$ of index two, for the internal coordinates, compare Table A2 in the appendix. One may imagine the start point after the SP$_{ca}$ at the allyl side, the NT then crosses the SP as a minimum on the way, and goes uphill the energy surface, see also Fig. 17 below. In the left panel of Fig. 6 we see that the NT has a returning behavior for the angle C2C1C3, at ≈81.5°. Note that the SP$_{i2}$ is in
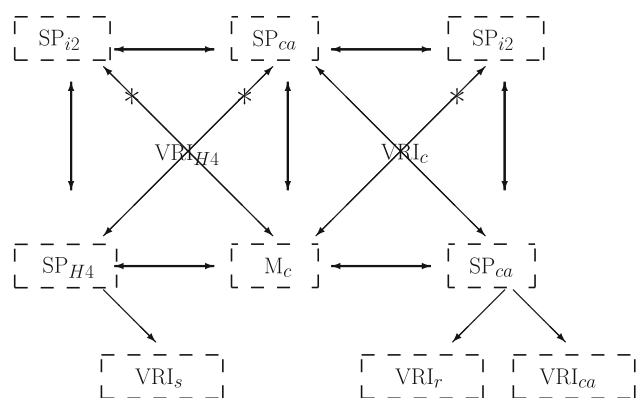
Scheme 1 Connection scheme of the cyclopropyl radical bowl. M_c: cyclopropyl radical minimum. SP_{ca}: TS of the ring opening of cyclopropyl radical to allyl radical. SP_{i2}: SP of index 2 where H_4 is in the CCC plane. The *two boxes* concern the same point. *VRI* valley-ridge inflection point of a singular NT between M_c and corresponding SPs. *Asterisk* depicts an intersection with another electronic surface; a systematic search by NTs breaks down. Corresponding NT arrows are hypothetical. The *lower line* of VRI points is outside the cyclopropyl radical bowl

the region of symmetry coordinates C_s, like M_c; however, it is not totally symmetric like M_a (the index a is used for the allyl radical minimum) with C_{2v} symmetry. For comparison, we also include the singular NT of VRI_c in Fig. 6. Its branches through the SP_{ca} should go, more or less, along the valley floor of the SP.

We also computed an NT which connects the SP_{i2} with the SP_{H4}, which is not shown in the Figs. 5 and 6. In Scheme 1 we collect the complete set of treated relations in the cyclopropyl radical bowl, compare also Fig. 17 below.

4 The SP_{ca} and the VRI_{ca} in the SP valley

The SP_{ca} associated with the ring opening of the cyclopropyl radical into the allyl radical is well known [25]. The coordinates at the UHF/6-31G(d) level of theory used in the present study are reported in appendix Table A1. The SP is not symmetric like the cyclopropyl or allyl radicals, compare Fig. 4. After the SP, with a further ring opening, there should be the post-TS bifurcation because at a possible end of the pathway one expects to find one of the diverse versions of an SP_{aa} in the allyl radical bowl, see

below; and due to this fact the downhill pathway flowing into the SP_{aa} region from SP_{ca} may be a ridge. At the beginning, the pathway is a valley. As an immediate consequence a VRI point must exist (Fig. 7).

To find this VRI_{ca} point was especially complicate, because the corrector of our method to follow NTs [8] does not properly work in the whole region around this VRI point. (Maybe because the determinant of the Hessian is very small, or because of any other reason.) See for comparison an example reported in [18] for the case of HCN with an analog but still worse behavior. Thus, we have to calculate the given NTs by predictor steps only using Branin-Euler steps along an equation of the tangent $\mathbf{x}' = \pm \mathbf{Ag}$. However, this does not mean to be a breakdown. Because near the VRI point, regular NTs are usually strong curvilinear but the searched VRI is usually outside of the convex region. Tangent steps in direction $\mathbf{x}'$ along such a curvilinear NT make their approximation error into the "right" direction. They lead nearer to the VRI point. If the VRI point is reached, the emergence of a cross of branches of the singular NT demonstrates the final success, see Figs. 8 and 9.

The electronic structure is very interesting because it represents the breakdown of the electronic state of the cyclopropyl structure, and it is the beginning of the unsymmetric region. The three important natural orbitals are shown in Fig. 7.

Every VRI system of a singular NT consists of four branches. The character of the single branches determines the character of the VRI point. The character of the VRI_{ca} is a branching of the uphill leading ridge from an hypothetical SP_{aa} region (being at the right-hand side, out of the Fig. 8) into two ridges going strong further uphill, and the one valley in between, which leads to the SP_{ca}. The character is an rpVRI of the chemically "interesting" case: between the bifurcating ridge-branches is the valley. (See below for singular NTs in not so "interesting" cases.) Thus, the ring-opening valley from SP_{ca} downhill ends at the VRI point. There are no bifurcating valleys downhill. Some authors name the situation of such an ending valley a "dangerous" bifurcation [41], or a bifurcation with indeterminate outcome, because further downhill after the VRI point, there the valley ground line disappears. After the VRI_{ca}, only the ridge-pathway continues further downhill. And going downhill on the PES, the ridge here shows a

Fig. 7 Natural orbitals of the VRI_{ca}: double-occupied with 1.723 occupation, single-occupied with 1.0 occupation, and un-occupied with 0.277 occupation
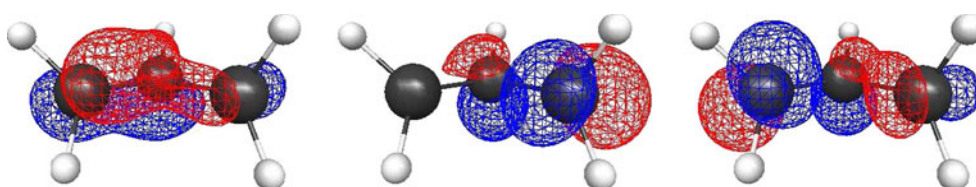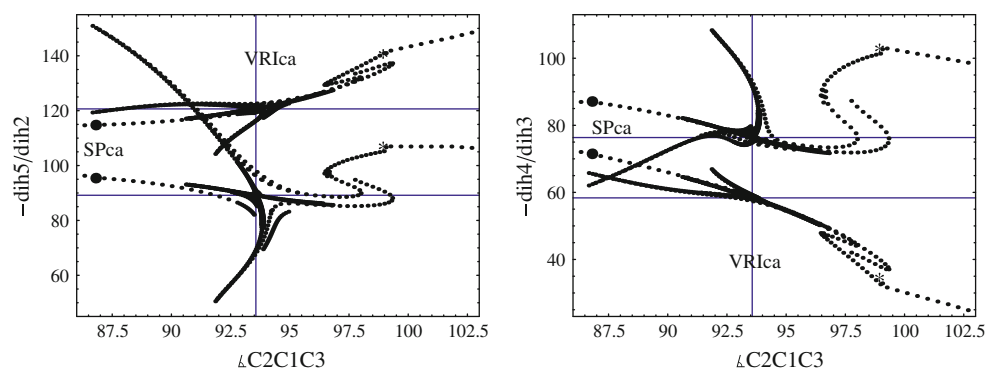
Fig. 8 VRI$_{ca}$ point behind the transition state, SP$_{ca}$, of the ring opening of the cyclopropyl radical. PES by UHF/6-31G(d). *Left* pieces of regular NTs around, as well as of the singular NT through the VRI$_{ca}$. Coordinates: angle between the C-atoms, and the two replaceable dihedrals dih2 and −dih5. The cross of the *three grid* *lines* is the location of the VRI point. The *asterisk* symbol again indicates the electronic intersection of a second PES of the allyl radical side of the problem. There, the current NT ends. The indicated here continuation is an artifact, at all. *Right* coordinates are the angle between the C-atoms, and the two dihedrals dih3 and −dih4, see text

Fig. 9 VRI$_{ca}$ for *Left* bond length coordinates r1 and r2 and *Right* dihedral dih1, see caption of Fig. 8. The inlay is VRI$_{ca}$
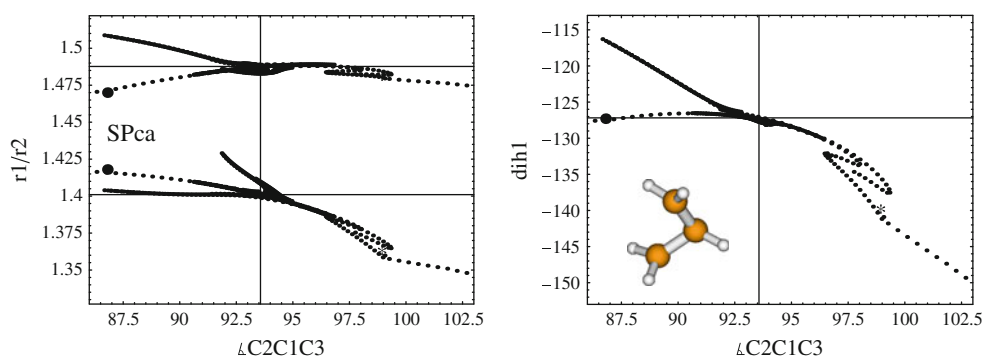
new effect, a "double bend" which indicates a road irregularity of the PES. A proposed explanation is added in the next Section.

The evolution pathway from SP$_{ca}$ to VRI$_{ca}$ includes quasi no change in the distance of the dihedral angles dhi3 and −dih4 in the right panel of Fig. 8. The two NTs are parallel. However, there is a small increase in the difference of dih2 and −dih5 (left panel of Fig. 8). The upper dihedral is increasing and the lower is decreasing. It means, the two upper hydrogens, H6 and H7 in Fig. 3, move disrotatory, where the two lower hydrogens, H8 and H5 in Fig. 3, move conrotatory along the left branch of the singular NT. The situation is changing drastically after the VRI point.

There, after VRI$_{ca}$ at the right-hand side in every of the two panels of Fig. 8, the branch of the singular NT is the crest of a ridge downhill. The double bend of this branch is quite different for either the methylene of C2 (dih2, −dih4), or the methylene of C3 (−dih5, dih3). Near 98° of the angle C2C1C3, there is a returning moment: methylene of C2 only stops, goes back, stops again and goes further to its aim. However, methylene of C3 fulfills a turn into a conrotatory direction. The distance (dih2 to −dih5) changes little; however, the distance (dih3 to −dih4) modifies very much.

Note that after the double bend of the NT there is the electronic intersection between PESs. One may speculate that this computed UHF PES will get ready for the crash by the tremor of the methylenes.

5 The effect of bumps in the road

There is a sudden change between disrotatory and conrotatory motion along some branches of the singular NT in a larger region of the PES, see Fig. 8 for the ridge after the VRI$_{ca}$ point. We demonstrate by a simple two-dimensional test surface, how such a road irregularity of NTs may emerge on a molecular PES. The left panel of Fig. 10 is calculated by the Mathematica® program. Such road irregularities emerge for NTs on the upper PES after the SP$_{ca}$ and can be seen when the curves are represented by bond angle C2C1C3 and dihedral dih2 shown in the right panel of Fig. 10. The possible additional small ridge on the PES then falls directly before the intersection of the PES related to another electronic state. The symbol * indicates here a precipice to a lower PES in the energy. We found that the UHF method is possibly not fully appropriate for the regions where the cliffs located between the plateau region of cyclopropyl radical

Fig. 10 *Left* 2D-test surface with an SP at (0,0), the SD from there (fat points), and a road irregularity for 5 NTs (*dashes*) passing the SP. The double bend of two connected turns that travel in alternate directions emerges by a very small, additional nose on the PES. It is produced by the function Exp$[-20\,(x + 0.5y - 1)^2]$ which is added to the saddle surface $3.5(x^2 - y^2)$. The steepest descent is much less disturbed than the NTs. *Right* Some NTs after SP$_{ca}$ with road irregularities
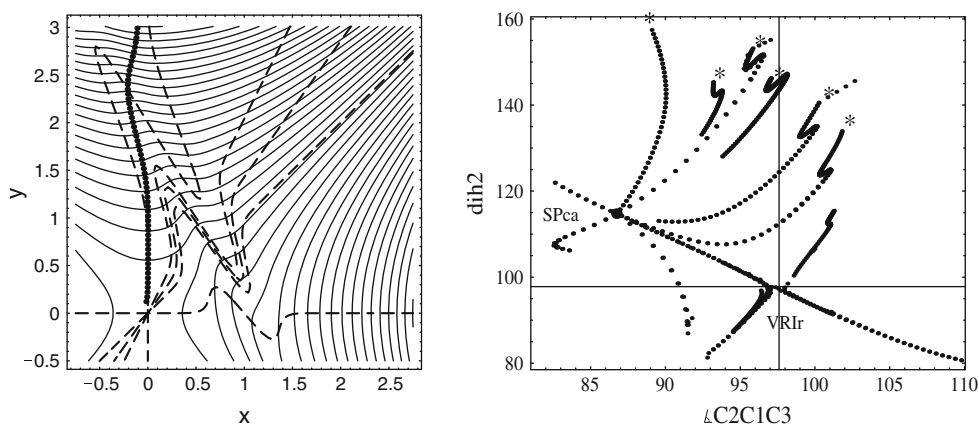
side, and the ground region of the allyl radical appear. Surprisingly, UHF does not converge in a suitable solution there. More specifically, the UHF solution gives a broken solution ($\langle S^2 \rangle$ is different from 0.75); however, it is not the correct solution that still is or should be a broken solution in the form that it is higher to 0.75. The UHF wave function possesses a set of UHF solutions in the region of the pronounced precipice, and one should take the correct solution: it is a task which is not easy. In fact the algorithm implemented in GAMESS-US [19, 20] package program to find the UHF in this case always converges to the non-appropriated solution. More explicitly, many times it converges either to the expected value for a pure doublet wave function solution ($\langle S^2 \rangle = 0.75$ or near it) or to the highest broken solution.

The intersection of the PESs itself is of the type "product side" [42], or, with another classification, of the type "peaked intersection" [35].

For some NTs, the nodes after the precipice indicate a continuation of the NT: that can be done by using the current gradient for the search direction of the new NT. Of course, it is not the continuation of the former NT, but it is a new one starting at the same point in coordinate space but with electronic structure of the lower surface. The gradients are quite different, usually, at the intersection of the two different surfaces. A systematic use of the NT theory is not possible if one overcomes the precipice.

6 Singular ridges on the upper PES (VRI$_r$, VRI$_s$)

In the right panel of Fig. 10, the next VRI point still near the SP$_{ca}$ is shown named VRI$_r$. It is on the upper UHF PES,

the PES of the cyclopropyl side. The UHF energy is -116.37204 au, see also Fig. 17 below, with $\langle S^2 \rangle = 1.517$. The occupancies of the natural orbitals ϕ_1 (being the orbital 11 in the natural orbital list), ϕ_2 (being the orbital 12), and ϕ_3 (being the orbital 13) are 1.507, 1.0, and 0.493, correspondingly. The occupancy reflects a strong delocalization in the electronic structure. It is due to the bond breaking between the atoms C2 and C3. A control calculation by the CASSCF method already shows a slow transition to a mix between π- and σ-electronic structure. The CASSCF energy of this point is -116.38154 au. The occupancies of the most important natural orbitals are for ϕ_1 (being the orbital 11 in the natural orbital list), ϕ_2 (being the orbital 12), and ϕ_3 (being the orbital 13) 1.1292, 1.0, and 0.8708, correspondingly. The S^2 operator commutes with the CASSCF Hamiltonian operator. It implies that for this energy functional the expectation value $\langle S^2 \rangle$ is always 0.75 for a doublet state.

The CASSCF result for the second root (electronic state) not optimized is located at ≈ 30 kcal/mol with respect to the ground state. It supports that the "upper" UHF wave function is appropriate in this region. But the VRI$_r$ point has more broken bonds than SP$_{ca}$, compare [25]. The structure of the orbitals can be found in Fig. 11. These orbitals are a mix between σ- and π-electronic structure. The movement of the first two eigenvectors of the Hessian matrix corresponds to a broken "symmetry C2C1C3 plane" in both directions, see below Fig. 22.

The VRI$_r$ defines a ridge system that divides NTs going downhill to SP$_{aa}$ (which is not shown) and other NTs going uphill into non-chemical mountains of the upper PES. We named it VRI$_r$, see Table A3 in the appendix, because it is

Fig. 11 Structure of CASSCF natural orbitals ϕ_1 to ϕ_3 (see text) at VRI$_r$
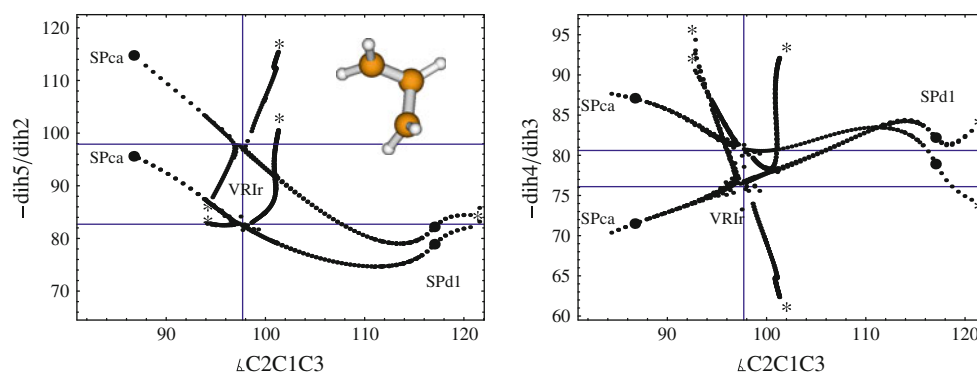
Fig. 12 *Left* branches of the singular NT through VRI$_r$ behind the transition state, SP$_{ca}$, on the upper electronic PES. Coordinates are the angle between the C-atoms, and the two dihedrals dih2 and −dih5. The cross of the *three grid lines* is the location of the VRI point. The *asterisk* symbol indicates again an electronic intersection of a second PES of the allyl radical side of the problem. The inlay is the shape of VRI$_r$. *Right* coordinates are the angle between the C-atoms, and the two dihedrals dih3 and −dih4. See text

a bifurcation of ridges [15]. Its character is an rpVRI. The singular NT of VRI$_r$ is depicted in Fig. 12. The central ridge connects two SPs, at the left-hand side the SP$_{ca}$ and at the right-hand side on the right the SP$_{d1}$, see Table 1 for its coordinates and energies. The symbol with $d1$ is used because the dihedral dih1 is mainly involved into the SP direction. In the left panel, that central ridge is the result of the bifurcation of a ridge being the branch left below of the VRI$_r$, and in the right panel it is the bifurcation of the branch left above. "Between" the two branches of the central ridge is the valley branch going here to the upper border of the left panel. On the PES it goes down in energy to the region of the SP$_{aa}$, see also Fig. 17 below. The valley branch in the right panel of Fig. 12 shows a different behavior: for dihedral dih3 it also goes up to the upper border; however, for dihedral −dih4 it goes to the lower border. It means that coordinates dih2 and −dih5 increase, and −dih4 decreases, quite in the same rate; however, −dih3 changes suddenly the direction at ≈100° of bond angle C2C1C3 and then increases strongly. The methylene of C2 turns in direction of the CCC plane, but the methylene of C3 is quenched, H6 against H8, first something disrotatory, then strong conrotatory.

The central ridge leads at the right-hand side of every panel from VRI$_r$ to the SP$_{d1}$. It can be characterized to be an SP of the H4 atom. It passes through the CCC plane there. The dihedral dih1 goes through 180°. It is still on the upper PES, at an energy of −116.37394 au; however, the H4-C1 has already the relation of the allyl radical structure. The four other dihedrals are quasi-symmetric; however, they are not fully symmetric. The movement along the branch from VRI$_r$ to SP$_{d1}$ is a decrease in dih2 and −dih5, but an increase in dih3 and −dih4; thus, it is a disrotatory rotation of the two methylenes.

The SP$_{d1}$ still belongs to the π-type radical electronic state (almost a ^{2}A' because this SP has C$_1$ symmetry). NTs

behind the SP$_{d1}$ meet again at an intersection with another electronic PES indicated by the * symbol.

A next VRI point on the upper surface is one between the SP$_{H4}$ of the M$_c$ bowl and again the region of the SP$_{d1}$. The point is named VRI$_s$ because it is in the symmetric subspace C$_s$ like the VRI$_c$. Its singular NT is a quasi-straight line in the coordinate space, and the angle dih1 remains throughout near −180°. It ends near the SP$_{d1}$ in an electronic intersection. The internal coordinates of VRI$_s$ are given in Table A3 in the appendix. The fractional occupancies of the natural orbitals are 2.0, 1.0, and 0.0. Thus, the avoided crossing seems to be far away. The UHF energy of VRI$_s$ is very high: −116.30119 au, see also Fig. 17 below. We think that it has no greater chemical meaning, without that to mark a high symmetry border between the chemical more interesting, unsymmetric regions of the PES. The singular NT is a ridge ascending from SP$_{H4}$. It bifurcates at VRI$_s$ into a symmetric ridge of index two, and two unsymmetric side branches (of index 1) which also quickly end at an intersection seam. This ridge ascending from SP$_{H4}$ is another one than the ridge ascending from SP$_{H4}$ to VRI$_{H4}$, compare Fig. 5.

7 Singular ridges on the lower PES (VRI$_{rl}$, VRI$_{i2}$)

One could speculate that a ridge on the lower PES, rising from SP$_{aa}$ in direction of SP$_{ca}$ under a decreasing bond angle C2C1C3, has to meet a VRI point where it transforms into a valley. But we could not find such a corresponding singular NT. Contrary, we found an uphill ridge from SP$_{aa}$ which meets a VRI$_r$ of the character rpVRI, but of a higher index, see Fig. 13. We named it VRI$_{rl1}$ with "r" because it is a bifurcation of ridges, "l" for the lower PES, and "1" for the first one, see below. Its coordinates are in Table A3 in the appendix. The character is a bifurcation of a usual
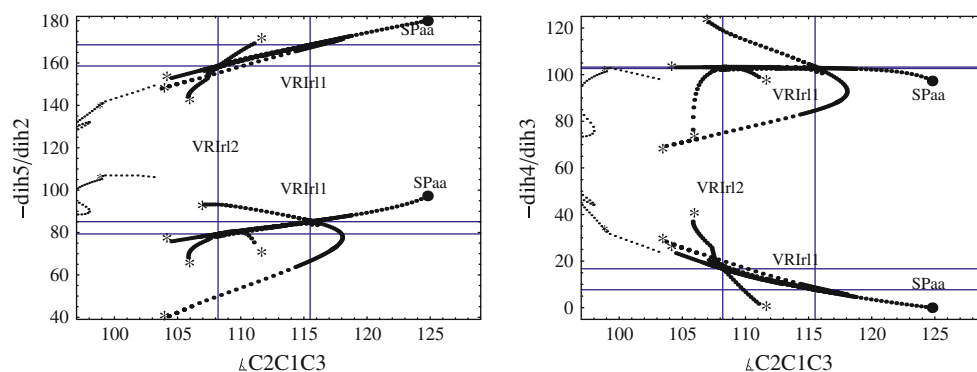
Fig. 13 *Left* singular NTs through two VRI_{rl} one after the other, on the lower PES, for coordinates dih2 and −dih5 against the angle C2C1C3. *Right* the same NTs for coordinates dih3 and −dih4. At the *left-hand side* of every panel are branches of the singular NT of the VRI_{ca}

Fig. 14 Natural orbitals of the SP_{i2}
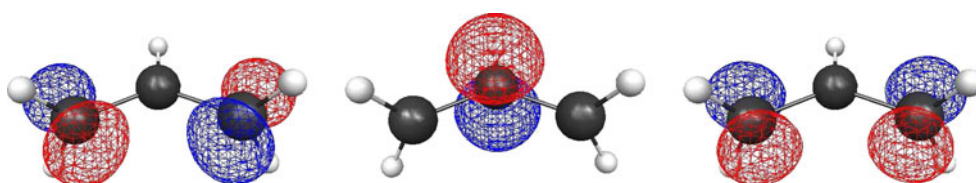
ridge of index one into two ridges of index one, and a ridge of index two in between, so to say a two-dimensional ridge on the 18-dimensional PES. Later, a further bifurcation happens at a VRI_{rl2} of the central ridge of index two into two ridges of index two, and a central ridge of index three, thus a ridge in tree dimensions. We guess that it is of less interest for chemical interpretations. Because, also its energy is high in the PES mountains. If one compares the corresponding branches with the system of branches of the VRI_{ca}, shown on the left-hand side by thinner points, it is clear that the two systems of VRI branches do not really fit together, though some single branches seem to meet.

On the central ridge of VRI_{rl1}, the dihedrals dih2 and −dih5 hold their distance over a ring closure of 20° of the bond angle C2C1C3 where they slightly decrease. The dihedral dih3 is constant, and dihedral −dih4 increases a little. The singular NT of the VRI_{rl1} corresponds to a quasi-disrotatory ring closure if it starts at SP_{aa}.

The full symmetric SP_{i2} of index 2 is also on the lower PES, however, already of an high energy of −116.37782 au. Its character is of σ-type radical electronic state ($^2A'$). It is in the coordinate space near to the SP_{d1} being on the upper PES, compare Fig. 12. Its character is of π-type radical electronic state (almost a $^2A''$ because this SP is C_1 symmetry). The UHF coordinates of SP_{d1} and SP_{i2a} are in Tables A4 and A5 in the appendix. Possible NTs between the two SPs cannot seriously be followed over the electronic intersection.

The SP structure of index 2 may clarify many aspects of the PES at first sight. The first eigenvector of the Hessian matrix at the point with the negative eigenvalue

corresponds to the conrotatory motion while the second one is disrotatory. We have done a comparison of the UHF geometry and their Natural Orbitals by a single-point calculation using the CAS(3x3) wave function, and it shows two almost degenerate electronic solutions. Maybe we are here in front of an intersection between the ground and the excited radical electronic states. It is important to take into account the conrotatory and disrotatory motion taking place in the excited state, see [25], and see the Section to the steepest descent from SP_{d1} below. The geometry of this SP of index 2 belongs to the C_{2v} point group of symmetry, see Fig. 14, the picture of the CAS Natural Orbitals with occupancies 0.774, 1.0, and 1.227, correspondingly.

Starting an NT on the lower PES at the SP_{i2}, this NT carries the index 2 from the beginning. We have also done that computational experiment hoping to loose some index. However, also such a singular NT, see Table A5 in the appendix, and Fig. 15, meets a VRI_{i2} with an rpVRI character of higher index. Here, the branch between SP_{i2} and the VRI_{i2} is a ridge of index 2. It bifurcates in two ridges of index 2, and a ridge of index 3 in between. It may be of lower chemical interest. The branch between SP_{i2} and the VRI_{i2} is still symmetric for the coordinate pairs dih2/ −dih5 and dih3/−dih4, correspondingly. The three uphill branches after the VRI point then show a splitting of these pairs of coordinates. Again, the symmetry of SP_{i2} is broken after the VRI_{i2}. The three forks of the ridge-pitchfork then rise up to non-interesting mountain regions of the PES. We guess that many further VRI points of higher index scrimmage in the region between SP_{aa} and SP_{ca}.
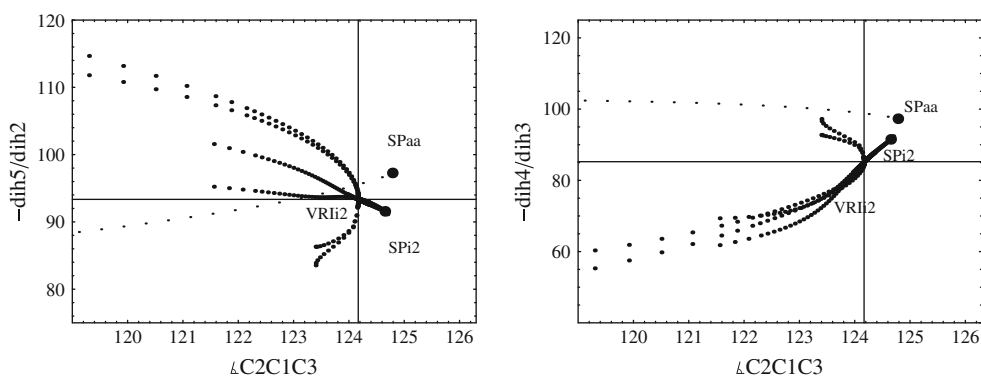
Fig. 15 *Left* singular NT through VRI$_{i2}$, for coordinates dih2 and $-$dih5 against the angle C2C1C3. *Right* the same NT for coordinates dih3 and $-$dih4. Thin points are from the right branch of a former

system of the singular NT of the VRI$_{rl}$, for comparison. Note that SP$_{i2}$ and SP$_{aa}$ are so closely related only in this projection
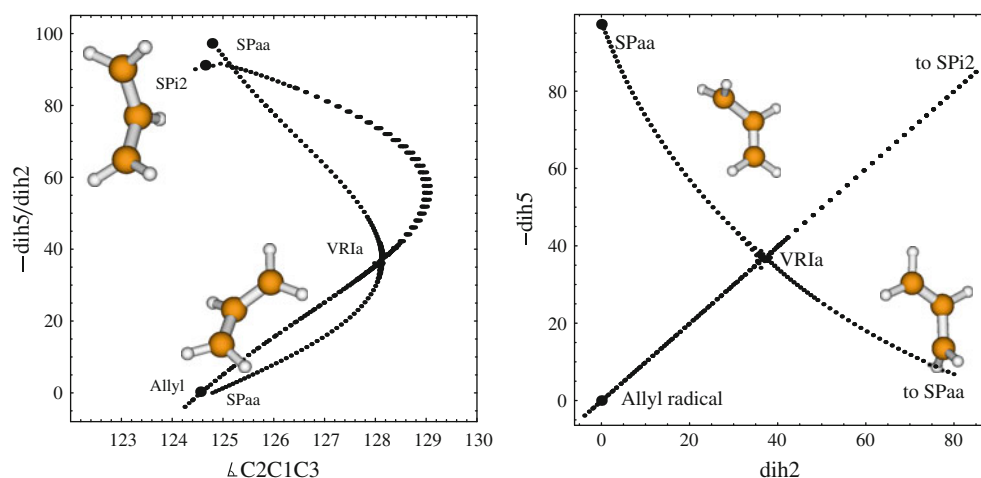
Fig. 16 *Left* singular NT through VRI$_a$ for coordinates dih2 and $-$dih5 against the angle C2C1C3. The small distances between SP$_{i2}$ and SP$_{aa}$, as well as between M$_a$ and SP$_{aa}$, come from the projection only which is used in the figure. The *upper* inlay is SP$_{i2}$, the lower inlay is VRI$_a$. *Right* the same NT for a direct comparison of the

coordinates dih2 and dih5. It shows the symmetry relation of the branches of the NT. (It may also give an impression of the importance of an appropriate projection for the understanding of a bifurcation.) The inlays are versions of SP$_{aa}$

8 The allyl radical bowl

The allyl radical minimum, M$_a$, is a well-known structure at many levels of theory [25], see also appendix, Table A6 for the full coordinates, and Table 1 for the reduced version.

Interesting points in the bowl of the minimum often belong to totally symmetric structures, see Fig. 2. A singular NT which starts at M$_a$ in the totally symmetric subspace of symmetry coordinates meets a VRI$_a$ point where the valley bifurcates into two valleys to two SPs named SP$_{aa}$, and a ridge in between to an SP of index two, SP$_{i2}$, see Fig. 16. The character of the VRI is a vpVRI. The UHF and CAS(3x3) calculations at VRI$_a$ coincide very much. The so-called "active space" (the electrons and orbitals which are strongly correlated) are those of the allyl radical minimum. The analysis of the eigenpair with null eigenvalue and orthogonal to the gradient vector reveals that it wants to move the

structure toward a methylene orthogonal to the CCC plane (C$_s$ point group of symmetry). The two SPs named SP$_{aa}$ are either the TSs of the rotation of the methylene related to C2, or of the rotation of the methylene of C3. The pathways to the two SPs are not totally symmetric, so that symmetry is broken at the VRI point named VRI$_a$. A curious fact is that the VRI$_a$ is reached with a further ring opening of the allyl radical (under a conrotatory motion of the terminal methylenes). Of course, the detection of the VRI$_a$ without a guess in this direction is not possible. It could be caught, nevertheless, by a temporary use of gradient extremals [15]. They are implemented in the GAMESS-US [19, 20].

A full picture of the description by NTs of the allyl radical bowl is shown in Scheme 2. Note: the scheme fully plays on the lower surface of the minimum bowl. Near SP$_{i2}$ one could think a transition to SP$_{d1}$ on the upper surface: it is a small step in the coordinate space, as well as by a small

Scheme 2 Connection scheme of the allyl radical bowl. M_a: allyl radical minimum; the *numbers* indicate the order of H atoms, see Fig. 3 which here is the *left, lower corner*. Methylene 1 is the *right group*, methylene 2 the *left group*. SP_{aa}: TS of the rotation of one methylene group, thus allyl to allyl TS. $m_i \perp$: the corresponding methylene i is quasi-orthogonal to the CCC plane. SP_{i2}: SP of index 2 where both methylenes are quasi-orthogonal to the CCC plane. VRI_a: branching point of the singular NT between M_a and SP_{i2}, and the two different SP_{aa}'s (see Fig. 16 for the NT). Of course, there is also one VRI_a in the three other quadrants, correspondingly

Fig. 17 Energies of the diverse points for the cyclopropyl radical to allyl radical ring opening

energy jump. However, the tool of NTs is not well adapted to the task. Only pieces of NTs on the different surfaces are possible, compare Fig. 21 below. The schematic energy profile over all interesting points is given in Fig. 17.

9 The examination of steepest descent from SP_{ca}

Last but not least, we report an SD calculation (without massweighting) through the interesting region after the SP_{ca} of the ring opening of cyclopropyl radical, see Figs. 18, 19 and 20. The SD curve runs after SP_{ca} the valley floor down and touches somehow the region of the VRI_{ca} point, compare Table A7 in the appendix where the SD node nearest to VRI_{ca} is reported. However, the dihedrals dih1 and dih3, as well as the bond length r2, do somehow deviate from the direct way to VRI_{ca}. Though the singular NT after the VRI_{ca} is the crest line of the ridge, in contrast, the SD runs below the ridge region after VRI_{ca} downhill, still along a valley region, to the intersection where the transition between pi-radical to sigma-radical electronic state occurs. The aim is the allyl radical surface, and the transition is symbolized by stars *. The SD jumps on a ridge region on the lower surface, at 106° of bond angle C2C1C3, and turns down along a flank, and later leaves the ridge region at the symbol) (. There it arrives at

the convex minimum region. The finish is that it ends at the minimum M_a with all dihedrals and bond lengths at the corresponding values.

The SP_{aa} direction is nearly met by the dih2/−dih5 couple after the VRI_{ca}. The single dihedral dih5 nearly touches the singular ridge NT belonging to VRI_{rl}, in this projection. But the near consistence of dihedrals dih2 and −dih4 with the central branch of the singular NT of the lower VRI_{rl} is only an accident of this projection. However, dihedral dih3 again goes the other way, as well as dihedral dih1 and bond length r2.

The judgment to go down to the minimum M_a, and not nearer to any version of the SP_{aa}, is rendered in the region around 106° of the bond angle C2C1C3, exactly at the electronic intersection. It becomes clear with the bond length coordinate r1 in Fig. 19. An indicator for an early turn down of the SD bypassing the region of SP_{aa} is also the profile of the energy along the SD, see Fig. 20. It seems that around 106° of the bond angle C2C1C3 are two jumps in the energy, one shortly after the other, see again the star symbols. It could mean that there are two intersections, at least on the UHF PES.

The SD curve corresponds after the SP_{ca} for dihedrals dih2, dih3 and dih4 to a quasi-disrotatory character. However, the dihedral dih5 alone behaves conrotatory. After the intersection around 106° of the bond angle C2C1C3, dih5 strongly changes the character and rotates exaggeratedly disrotatory. This is in accordance with the twofold intersection event [43]. But, the SD pathway shows no unique behavior, compare [44]. At all, the SD seems to be "navigated" by the singular NTs of the different VRI points. At the beginning, as one expects, the SD follows the valley into the region of VRI_{ca}. And after the VRI_{ca}, it goes down bordered by the different singular ridges. However, the SD does not feel the bumps of the PES like the corresponding branch of the singular NT through VRI_{ca}. At

Fig. 18 Fat nodes indicate the steepest descent from SP_{ca} to allyl radical minimum. The *asterisk* symbol is the intersection to the PES of the allyl radical minimum, and the symbol) (means the border from ridge region to valley region near 120° of bond angle C2C1C3. NTs of thin points are the former systems of VRI_{ca} and VRI_{rl}, for comparison, see Figs. 8 and 13. Note that the used projection sees the allyl and one version of SP_{aa} at the same place. *Left* coordinates dih2 and −dih5, *right* coordinates dih3 and −dih4
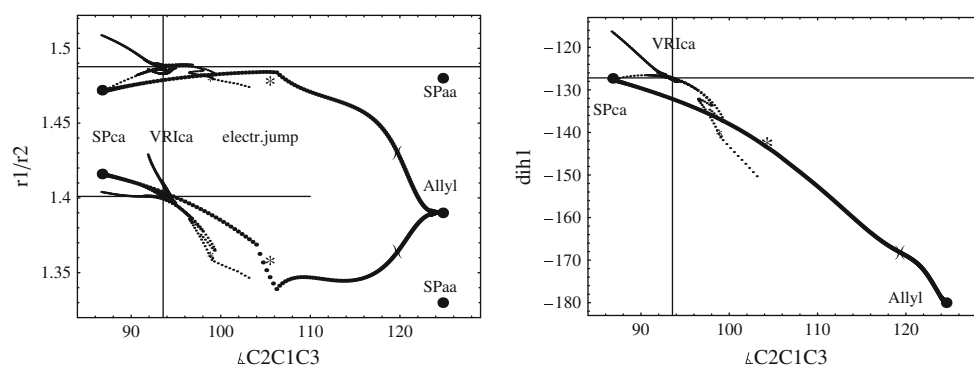
Fig. 19 Steepest descent from SP_{ca} to allyl radical minimum. See caption of Fig. 18. *Left* coordinates r1 and r2, *right* coordinate d1
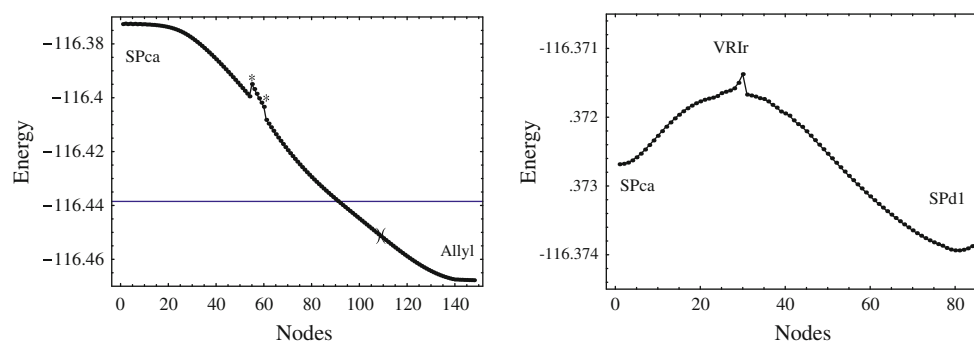
Fig. 20 *left* energy profile along the SD from SP_{ca}. The *two asterisks* symbols two times indicate an electronic intersection of the UHF PES. The *grid line* is at the energy of the SP_{aa}. *Right* example of an energy profile along two branches of the singular NT from SP_{ca} over VRI_r to SP_{d1}, see Figs. 12 or 21. The peak emerges by the jump from one (not perfectly singular) branch to the next one

the end, the final allyl radical minimum, M_a, is connected to M_c and SP_{ca} by a disrotatory change [26]. Because of the intersection seam that crosses the descent region after the VRI_{ca}, and which is represented by a steep precipice, the flow of SD lines from different beginnings (slightly "left" or "right" from VRI_{ca}, see also the next section) finds always the disrotatory allyl radical minimum. So to say, the VRI_{ca} point is relegated to uselessness by the lower electronic surface of the allyl radical side.

Technically, the SD calculation is done by simple Euler steps along the normalized contravariant gradient. The steplength used is 0.05 units (in the Bohr/radiant system). Because no further numerical effort is taken into account (compare, for example, [45]), there is some mild zigzagging, at the beginning in the SP region, as well as in the region of the minimum. However, the overall picture is not perturbed by this effect, especially because of the very small steplength.

10 The steepest descent from VRI$_r$ and SP$_{d1}$

The corresponding SD curves are depicted in Fig. 21. The VRI$_r$ is at the slope of the PES, and the SD from there goes down into the bowl of the minimum of the disrotatory allyl radical. At the other side, the two SD curves (and one for every dihedral in our double representation) run from SP$_{d1}$ in two opponent directions along the 1-dimensional valley floor down, and they find two different allyl radical mini-mums, either one of a disrotatory or one of a conrotatory structure.

The pathway of the SD in Fig. 21 is near the SP$_{d1}$ a rotation of one single methylene. The other methylene stays at the point and does not move. Thus, the SD is a pathway in direction to an SP$_{aa}$. However, after $\approx 35°$ of rotation, the intersection seam to the allyl radical surface is crossed. There the second methylene starts also a rotation and the radical goes down to the allyl minimum. In Fig. 21, left panel, the "upper" SP$_{d1}$ belongs to coordinate dih2, but the "lower" SP$_{d1}$ belongs to −dih5. The both col directions of the SP go along the pure dih2 (and not shown, a part of dih1 coordinate). A similar picture is the right panel, where dih3 is the active coordinate, but −dih4 stays. From point of view of the theory of NTs, there has to be a VRI point between SP$_{d1}$ and SP$_{aa}$. We have done some search, but did not find it. The intersection seam again disturbs the pure theory of an NT-connection of the both SPs.

The SP$_{d1}$ is the outpost of the cyclopropyl radical side, of the upper surface. It is the "upper complement" to the SP$_{i2a}$ on the allyl radical side, the σ-type radical electronic surface. One may speculate that there is also an SP$_{i2u}$ on the upper surface near the two SPs of index one, SP$_{d1}$. Because, the relations of the two special points are dif-ferent: For the methine bond, C1H4, the SP$_{d1}$ is a maxi-mum at 180°, but the SP$_{i2a}$ is a minimum. For the (quasi orthogonal to the C2C1C3 plane) dihedrals of the two methylenes, the SP$_{d1}$ is a maximum for the rotation of one methylene, but a (very flat) minimum for a conrotatory

rotation of both methylenes, but the SP$_{i2a}$ is the twofold maximum for the methylenes rotation. One eigenvector of the Hessian matrix with negative eigenvalue corresponds to the conrotatory motion while the second one is disrotatory. The direction of the SP valley of the SP$_{d1}$ is a linear combination of the H4C1 bond vibration, and the rotation of only one methylene. So, the different index is explained. The points SP$_{d1}$ and SP$_{i2a}$ are adjacent points, in coordinate space, as well as in their energy. But of course, between the two special points is the intersection seam. So, we can draw NTs between them, but they would cross the precipice. In Fig. 21, at the right-hand side in every panel, the NT is continued over the SP$_{d1}$ uphill, and then down the precipice to SP$_{i2}$. In contrast to this direction is the SD from SP$_{d1}$. It starts orthogonally in direction to an SP$_{aa}$. The two sym-metric forms of SP$_{d1}$ are characterized by a difference of only 3.3° of the dihedrals of the two methylenes. However, this small difference is crucial for two very different directions of the corresponding SP cols in Fig. 21. From point of view of the theory, there has to be a further SP$_{i2}$ between the two SPs$_{d1}$ also on the upper surface. We have done some search, but we did not find it. The intersection seam disturbs this search.

The results are collected in Scheme 3. May be Scheme 3 and Fig. 21 can explain the trajectory results of Mann and Hase [27, 28].

In Fig. 22 we show the first two eigenvectors of the Hessian at VRI$_r$. The direction of the eigenvector with zero eigenvalue points to the two SPs. The gradient leads to the structure where the unpaired electron is located in the plane C2C1C3 corresponding to the electronic state ^{2}A'. The VRI$_r$ is at the slope of the PES, but the slope is small. Note that the singular branch to SP$_{d1}$ is a ridge line, but it does not need to be the crest line. We may assume that a dynamical trajectory can overfly the VRI$_r$ region. When such a dynamical trajectory glides with high velocity over the VRI$_r$ and runs further along, or near, the branch of the singular NT to SP$_{d1}$, then it has the possibility to slide
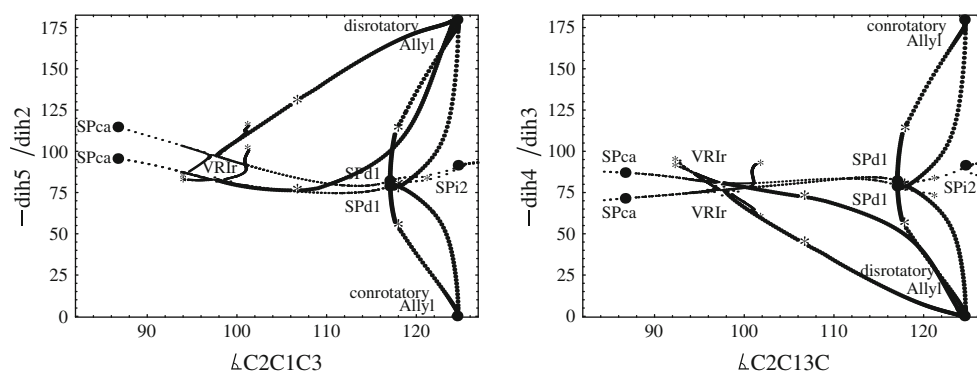
Fig. 21 Steepest descent (*bullets*) from VRI$_r$ and SP$_{d1}$ to two versions of the allyl radical minimum. Thin points are the singular NT of VRI$_r$. *Left* coordinates dih2 and −dih5, *right* coordinates dih3 and −dih4
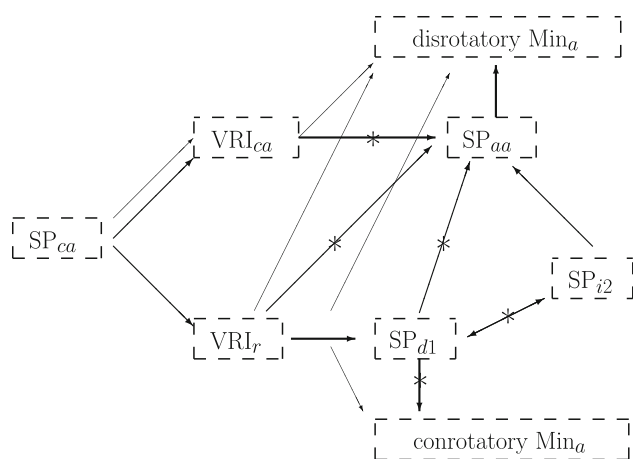
Scheme 3 Possible flow of singular NTs (*thick arrows*) and some SD lines (*thin arrows*) for the ring opening after SP_{ca}. (For symbols see the Captions of former schemes.) *Asterisk* depicts an electronic intersection. Corresponding arrows for NTs are drawn only symbolically. In contrast, SD lines can jump down and continue after the intersection seam

down at the "conrotatory" side of the flat ridge which itself leads to SP_{d1}. So to say, the branch of the singular NT from VRI_r to SP_{d1} is a kind of a TS demarcation line [46]. If it is overcome then the conrotatory side of the PES is possible. The VRI_r does not be an obstacle. It is only a little higher in energy than the SP_{ca}, and the ridge from VRI_r goes very slowly down to SP_{d1}, see the energy profile in the right panel of Fig. 20. The ridge to SP_{d1} is throughout on the upper electronic PES. A hypothetical, dynamical trajectory could connect the SP_{ca} with the minimum of the conrotatory structure of the allyl radical, being a result of Mann and Hase [27, 28].

A qualitative similar PES situation was found for another reaction system

$$CH_3O \leftrightarrow H_2 + HCO \leftrightarrow H + H_2CO.$$

A two-dimensional section of the corresponding PES is depicted in Fig. 4 of [47]. The reaction was named a reaction over a barrier but not through an SP. Further examples of reactions, which do not follow the post-TS IRC, are reported [48–52]. Of course, a reaction which
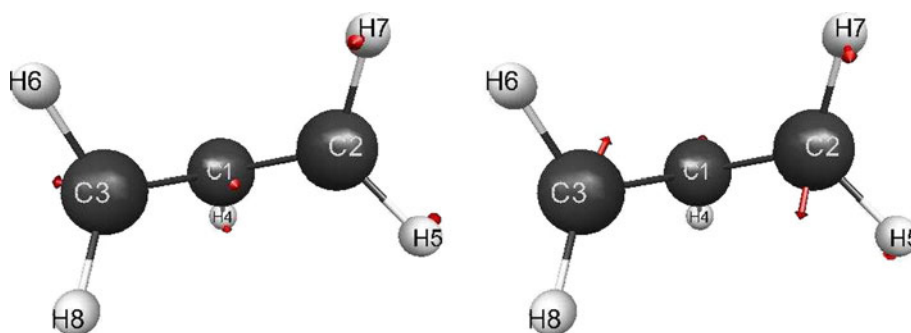
does not follow the post-TS IRC is not so easy to explore with the tool of SD curves [47]. It could be explored better if one uses the tool of NTs.

11 Discussion

The PES of the ring opening of the cyclopropyl radical is notoriously curvilinear. To see anything at all, we concentrate our interest to projections to the 5 dihedrals, and the two distances of the C-atoms of the 8-atomic molecule. It may be problematic to treat only these projections: there are still 5 distances and 5 angles of the H atoms not treated here (except in the reported tables in the appendix).

We have tested the reliability of the use of the UHF PES by calculation of the corresponding CASSCF energies of representative points of the UHF PES. The results in Table 2 show an energy difference that is constant for nearly all the points, meaning that UHF underestimates the energy about 8-9 kcal/mol. Only for some points being near to the electronic intersection this energy difference raises above 10 kcal/mol. This demonstrates, that UHF is a good approximation, as there is a constant error, and not an error depending on the current point. Curiously, the UHF PES around the symmetric SP_{i2} of the allyl bowl has a strange energy difference, as well as the quasi-symmetric SP_{d1}. The energy calculated at the UHF level is lower than that of the CAS calculation, but this, although unusual, is possible mathematically. The reason is that here the quadruplet electronic state (occupation 1.0, 1.0, 1.0) using UHF wave function for the energy is lower with respect to the doublet state and CASSCF. It means that in this region the quadruplet electronic state is the lowest electronic state rather than the doublet state. In others words, in this region the calculation of CASSCF corresponds to an excited state.

12 Conclusion

With this work, we open the possibility to channelize the ring opening of the cyclopropyl radical between some

Fig. 22 *left* zero eigenvector at VRI_r. It points along the two branches from SP_{ca} to SP_{d1} and marks the level line of curvature zero. *Right* second eigenvector in direction of the gradient at VRI_r. It points along the other two branches

Table 2 Comparison of UHF and CAS energy values of representative UHF points with basis set 6–31 G(d)

Point	Energy UHF au	Energy CAS au	Difference[a] kcal/mol
M_c[b]	−116.41492	−116.42759	7.95
VRI_c	−116.37773	−116.39038	7.94
SP_{H4}	−116.40935	−116.42106	7.35
SP_{i2c}	−116.34794	−116.36014	7.66
SP_{ca}	−116.37268	−116.39261	12.51
VRI_{ca}	−116.37565	−116.39027	9.17
VRI_r	−116.37204	−116.38154	5.96
VRI_s	−116.30119	−116.31365	7.82
IRC_1	−116.37819	−116.39204	8.70
IRC_2	−116.39950	−116.42460	15.75
SP_{d1}[c]	−116.37394	−116.36720	−4.23
SP_{i2a}	−116.37782	−116.35932	−11.61
IRC_3[d]	−116.41226	−116.43681	15.41
VRI_{rl1}	−116.42231	−116.44542	14.50
SP_{aa}	−116.43851	−116.46178	14.60
VRI_a	−116.44217	−116.45563	8.45
M_a	−116.46810	−116.48358	9.71

[a] Factor: 1 au = 627.509 kcal mol^{-1}

[b] The upper table concerns the PES of the cyclopropyl radical side

[c] See text for the negative differences

[d] The lower table concerns the PES of the allyl radical side

singular NTs. The known SP of the ring opening, SP_{ca} [25], is now included in a row of VRI points, as well as SPs of index 2, on the UHF PES. The tool to find these special points is a variational application of Newton trajectories (NT) proposed in [18].

The breakdown of the symmetry of the cyclopropyl radical, or the allyl radical takes place at the pre-transition state VRI point, VRI_c, and at point VRI_a. Up to these two points, a possible reaction path coming from the minimums could be thought to be fully symmetric. But the transition states SP_{ca} and SP_{aa} are not symmetric, and so the branches leading to these SPs have to be not symmetric as well. The corresponding archetypes are Fig. 4 left panel, and Fig. 16 right panel. Of course, any "direct" pathway between minimum M_c and SP_{ca}, for example, can be a model of the reaction path including the SD from SP_{ca}. The singular NT through the VRI_c only marks a border for such RP models marking a so-called reaction channel [53–55].

After the SP_{ca} of the ring opening, and before the adjacent SP_{aa} in the allyl bowl, has to be at least one further VRI point. We propose to assume the VRI_{ca} for that event. However, the case of electronic intersections of different PESs disturbs a usual application for this molecule of the NT theory concerning the existence of VRI points in certain relations between the stationary points

[8, 9]. Rising uphill from SP_{aa} or SP_{i2a}, correspondingly, we found further "systems" of VRI points of rpVRI character of higher index. Their singular NTs may not directly lead to SP_{ca}, and they are lost somewhere in the PES mountains of non-chemical high energies. However, they narrow the region where one can guess the pathway of the ring opening. This is demonstrated by a SD calculation, at least, which finds its way through the different singular NTs. These set the limits for the SD form SP_{ca} to M_a.

On the other hand, the use of SD separates the different interesting points of the PES (SPs, VRI points) into different regions of attraction of the dis or conrotatory minimums. The ring opening shows a very mixed character of con and disrotatory motion of the methylenes if one traces the different singular NTs, as well as the SD from SP_{ca}. Thus, the question of the character of the ring opening is that neither a clear conrotatory nor a clear disrotatory motion takes place [44]. The summary result of NTs or SD from SP_{ca} down the SP valley is the disrotatory minimum. However, the singular NT along a ridge region from SP_{ca} to SP_{d1} could explain a possibility for a conrotatory ring opening. Thus, the diverse singular NTs set the limits for usual static reaction pathways. But they may open the insight for results of dynamical trajectories, compare [27, 28], where some trajectories go to a conrotatory ring opening.

A side result in this work is the assignment of a so-called mixed character VRI point on the PES of a real molecule, the VRI_{H4}. The kind of VRI point was recently described [15, 17]. A further side result in this work is the detection, and possible meaning of so-called bumps on the PES. They are indicated by double bends of the NTs, see Fig. 10.

With the reaction of the cyclopropyl radical ring opening to allyl radical, we have shown that the NT methodology provides a tool to explore the topology of the potential energy surface. The so-called singular Newton trajectories acquire special importance. These curves pass through the VRI points and the corresponding analysis of each branch that crosses the VRI provides information on the structure and form of the surface around this point. They are related with the bifurcation of valleys. This work also seeks to pave the way to further fruitful applications of the mathematics of VRI points and the bifurcation of NTs in other molecules.

References

1. Mezey PG (1987) Potential energy hypersurfaces. Elsevier, Amsterdam

2. Heidrich D (ed) (1995) The reaction path in chemistry: current approaches and perspectives. Kluwer, Dordrecht
3. Fukui K (1970) J Phys Chem 74:4161
4. Hofmann DK, Nord RS, Ruedenberg K (1986) Theor Chem Acta 69:265
5. Sun J-Q, Ruedenberg K (1993) J Chem Phys 98:9707
6. Quapp W (1989) Theor Chem Acta 75:447
7. Williams IH, Maggiora GM (1982) J Mol Struct 89:365
8. Quapp W, Hirsch M, Heidrich D (1998) Theor Chem Acc 100:285
9. Quapp W, Hirsch M, Imig O, Heidrich D (1998) J Comput Chem 19:1087
10. Quapp W (2001) J Comput Chem 22:537
11. Hirsch M, Quapp W (2002) J Comput Chem 23:887
12. Anglada JM, Besalú E, Bofill JM, Crehuet R (2001) J Comput Chem 22:387
13. Bofill JM, Anglada JM (2001) Theor Chem Acc 105:463
14. Crehuet R, Bofill JM, Anglada JM (2002) Theor Chem Acc 107:130
15. Quapp W (2004) J Molec Struct 695(-696):95
16. Valtazanos P, Ruedenberg K (1986) Theor Chim Acta 69:281
17. Bofill JM, Quapp W (2011) J Chem Phys 134:074101
18. Quapp W, Schmidt B (2011) Theor Chem Acc 128:47
19. Schmidt MV, Baldridge KK, Boatz JA, Elbert ST, Gordon MS, Jensen JH, Koseki S, Matsunaga N, Nguyen KA, Su S, Windus TL, Dupuis M, Montgomery JA Jr (1993) J Comput Chem 14:1347
20. Gordon MS, Schmidt MW (2005) In: Dykstra CE, Frenking G, Kim KS, Scuseria GE (eds) Theory and applications of computational chemistry, the first forty years, chap 41. Elsevier, Amsterdam, p 1167 (GAMESS Version 2007)
21. Quapp W (2010) web-page: http://www.math.uni-leipzig.de/~quapp/SkewVRIs.html
22. Woodward RB, Hoffmann R (1965) J Am Chem Soc 87:395
23. Woodward RB, Hoffmann R (1969) Angew Chem Int Ed Engl 8:781
24. Clark DT, Adams DB (1971) Nature Phys Sci 233:121
25. Olivella S, Solé A, Bofill JM (1990) J Am Chem Soc 112:2160
26. Arnold PA, Carpender BK (2000) Chem Phys Lett 328:90
27. Mann DJ, Hase WL (2002) J Am Chem Soc 124:3208
28. Mann DJ, Halls MD (2002) Phys Chem Chem Phys 4:5066
29. Aguilar-Mogas A, Giménez X, Bofill JM (2010) J Comput Chem 31:2510
30. Lucas JM, de Andrés J, Albertí M, Bofill JM, Bassi D, Aguilar A (2010) Phys Chem Chem Phys 12:13646
31. Pulay P, Hamilton TP (1988) J Chem Phys 88:4926
32. Bofill JM, Pulay P (1989) J Chem Phys 90:3637
33. Arnold PA, Cosofret BR, Dylewski SM, Houston PL, Carpenter BK (2001) J Phys Chem A 105:1693
34. Yarkony DR (1996) Rev Mod Phys 68:985
35. Martinez TJ (2010) Nature 467:412
36. Holtzhauer K, Cometta-Morini C, Oth JFM (1990) J Phys Org Chem 3:219
37. Dong F, Davis S, Nesbitt DJ (2006) J Phys Chem 110:3059
38. Hirsch H, Quapp W, Heidrich D (1999) Phys Chem Chem Phys 1:5291
39. Quapp W, Hirsch M, Heidrich D (2004) Theor Chem Acc 112:40
40. Pechukas P (1976) J Chem Phys 64:1516
41. Thompson JMT, Stewart HB, Ueda Y (1994) Phys Rev E 49:1019
42. Robb MA, Olivucci M (2001) J Photochem Photobiol A 5373:1
43. Longuet-Higgins HC, Abrahamson EW (1965) J Am Chem Soc 87:2045
44. Schultz T, Clarke JS, Gilbert T, Deyerl H-J, Fischer I (2000) Faraday Discuss 115:17
45. Hratchian HP, Schlegel HB (2004) J Chem Phys 120:9918
46. Voth GA, Hochstrasser RM (1996) J Phys Chem 100:13034
47. Knyazev VD (2002) J Phys Chem A 106:8741
48. O'Neal D, Taylor H, Simons J (1984) J Phys Chem 88:1510
49. Sun L, Song K, Hase WL (2002) Science 296:875
50. Debbert SL, Carpender BK, Hrovat DA, Borden WT (2002) J Am Chem Soc 124:7896
51. Ammal SC, Yamataka H, Aida M, Dupuis M (2003) Science 299:1555
52. López JG, Vayner G, Lourderaj U, Addepalli SV, Kata S, deJong WA, Windus TL, Hase WL (2007) J Am Chem Soc 129:9976
53. Hirsch M, Quapp W (2004) J Mol Struct 683:1
54. Hirsch M, Quapp W (2004) J Math Chem 36:307
55. Quapp W (2009) J Theor Comput Chem 8:101